Defence Technology 16 (2020) 1106–1115

Contents lists available at ScienceDirect

Defence Technology

journal homepage: www.keaipublishing.com/en/journals/defence-technology

Experimental research on the instability propagation characteristics of liquid kerosene rotating detonation wave

Quan Zheng, Hao-long Meng, Chun-sheng Weng*, Yu-wen Wu, Wen-kang Feng, Ming-liang Wu

National Key Laboratory of Transient Physics, Nanjing University of Science and Technology, Nanjing, 210094, China

ARTICLE INFO

Article history:
Received 6 May 2020
Received in revised form
27 May 2020
Accepted 23 June 2020
Available online 3 July 2020

Keywords:
Rotating detonation wave
Liquid kerosene
Oxygen-enriched air
Instability propagation characteristics
Compression wave

ABSTRACT

In order to study the instability propagation characteristics of the liquid kerosene rotating detonation wave (RDW), a series of experimental tests were carried out on the rotating detonation combustor (RDC) with air-heater. The fuel and oxidizer are room-temperature liquid kerosene and preheated oxygen-enriched air, respectively. The experimental tests keep the equivalence ratio of 0.81 and the oxygen mass fraction of 35% unchanged, and the total mass flow rate is maintained at about 1000 g/s, changing the total temperature of the oxygen-enriched air from 620 K to 860 K. Three different types of instability were observed in the experiments: temporal and spatial instability, mode transition and re-initiation. The interaction between RDW and supply plenum may be the main reason for the fluctuations of detonation wave velocity and pressure peaks with time. Moreover, the inconsistent mixing of fuel and oxidizer at different circumferential positions is related to RDW oscillate spatially. The phenomenon of single-double-single wave transition is analyzed. During the transition, the initial RDW weakens until disappears, and the compression wave strengthens until it becomes a new RDW and propagates steadily. The increased deflagration between the detonation products and the fresh gas layer caused by excessively high temperature is one of the reasons for the RDC quenching and re-initiation.

1. Introduction

Detonation is a supersonic combustion phenomenon characterized by the coupling of a shock wave with the reaction front behind it [1]. Compared to deflagration, detonation results in greater intensity of heat release and smaller entropy increase. The theoretical efficiency of the thermodynamic cycle based on detonation can be improved by nearly 20–50% when compared with the classical Brayton cycle [2]. The rotating detonation engine (RDE) is a novel propulsion concept which utilizes one or multiple detonation waves propagating around the annular channel continuously to produce steady thrust [3–5]. The RDE is generally equipped with an annular combustion chamber, and the fresh propellants are injected from the head-end of combustion chamber. The rotating detonation combustor can be applied to all kinds of propulsive engines including rocket, ramjet, turbine, and combined-cycle engines. Due to the its huge potential, RDE has received increased attention over the past few years [6,7].

Over the past decade, significant progress has been made in the research and development of RDC, such as rotating detonation structure and dynamics [8–11], the different geometrical configurations of RDC [12–15], injection and mixing [16–18], mode of operation at off-design conditions [19–23], and the feedback of RDW on the reactant plenums [24–26]. Researchers have revealed that the basic operating modes of RDC are also identified-steady single wave [27–32], single wave and multiple waves alternation [28,31,32], steady multiple waves [27,29–32], and multi wave collision [28,30,32]. Moreover, various types of detonation instability phenomena in the H_2/air RDC was observed such as chaotic, low frequency oscillations, mode transition and longitudinal pulsed detonation. Existing research has shown that most of the previous study on RDC has been focused on gaseous fuels. However, for practical applications, the liquid fuel could be more attractive due to its higher energy density and ease of storage [17].

Kindracki et al. [16,33] used a propellant of the hydrogen-

* Corresponding author.
E-mail address: wengcs@126.com (C.-s. Weng).
Peer review under responsibility of China Ordnance Society

https://doi.org/10.1016/j.dt.2020.06.028

kerosene-air for rotating detonation experiments. When the air mass is 320 g/s the hydrogen is 10 g/s and the kerosene mass flow rate is 16.5 g/s, and the equivalent ratio is 1.1, a self-sustained RDW with a propagation velocity of 1500 m/s is achieved. Bykovskii et al. [34,35] described experimental research for liquid kerosene with oxidizer (50% O_2 and 50% N_2) in a detonation chamber. They also used a mixture of propane and air and compared results against a kerosene mixture. Zheng et al. [37] experimentally studied influence of the equivalence ratio on the propagation characteristics of detonation waves with gasoline-oxygen-enriched air, and the propagation velocity was 1022.2–1171.8 m/s. Zhong et al. [38,39] investigated the rotating detonation supplied by the pre-combustion cracked kerosene with oxygen-enriched air. In addition, the effect of the channel and injection slot width for oxidizer on the rotating detonation wave was researched. Li et al. [17] investigated the feasibility and operability of liquid-fuel RDC using JetA-1 with premixed and non-premixed injection strategies. The results confirmed that the measured concentration was indeed higher than the upper explosive limit. Compared to gaseous fuels, technical challenges that exist in liquid fuel rotating detonation engine are more crucial. Not only the evaporation and atomization of liquid fuel, the mixing of fuel and oxidant, but also the physical and chemical properties of fuel itself (chemical reaction activity, temperature, etc.) need to be considered.

In general, stable rotating detonation with predictable and stable pressure peaks is always desirable. Strong unstable rotating detonation pressure flow can have undesired effects on combustor, propellant supply system, and engine performance. Unfortunately, unstable rotating detonation is widespread in both gas [20,22] and liquid [16] fuels. In order to improve the stability of the rotating detonation engine, a variety of methods have been tested, including the use of oxygen-enriched air [36,40], changing the combustor geometry [34,41], injection parameters [42,43], and heating of the reactants [38,39]. Although detonation stability is a necessary condition for the practical application of two-phase RDC, there is a paucity of studies on it.

In this paper, the propagation characteristics of liquid kerosene rotating detonation wave at different total temperatures of oxygen-enriched air is studied experimental by using a RDC with air-heater. Three different types of instability were observed in the experiments: temporal and spatial instability, mode transition and re-initiation. Through the analysis of the experimental results, the instability propagation mechanism of liquid kerosene RDW under the condition of high temperature oxygen-enriched air is obtained.

2. Experimental facility and methodology

As shown in Fig. 1, the experimental system consists of two-phase RDC, combustion air-heater, propellants delivery system, control and data acquisition system, and ignition system.

2.1. Experiment facility

The physical configuration of RDC model with air-heater is shown in Fig. 2. The air-heater is composed of combustor, oxygen supplement section, honeycomb mixing section and measuring section. In the air-heater, firstly, the total temperature of the air is increased by burning hydrogen, and then the oxygen is supplemented to the required oxygen mass fraction through the four intake holes, and then blended through the honeycomb mixing section to ensure uniform temperature and oxygen mass fraction distribution. The measuring section is equipped with four temperature sensors and four oxygen sensors in the circumferential direction, and each sensor is at a different distance from the center of the mixing section to ensure that the high-temperature oxygen-enriched air has the same temperature and oxygen mass fraction in different circumferential positions before entering the detonation combustor. The change of the total temperature of oxygen-enriched air is achieved by adjusting the mass flow of hydrogen and oxygen.

A pre-detonator is used as the ignition device, which is tangentially connected to the annular combustor, as shown in Fig. 3(b). The pre-detonator uses hydrogen and oxygen, injected in a non-premixed manner, and ignited by a spark plug. A Shchelkin spiral is used to facilitate the deflagration-to-detonation (DDT) process. The detonation wave enters into the annular combustor and induces the detonable mixture in the annular combustor to develop into RDW.

The room-temperature liquid kerosene is selected as fuel and the oxygen-enriched air is the oxidizer. The inner diameter, outer diameter, the width and length of annular combustor are 120 mm, 153 mm, 16.5 mm and 210 mm, respectively. All propellant pipes are controlled by reduction valves, electromagnetic valves and check valves to ensure relatively stable flow for the experiment.

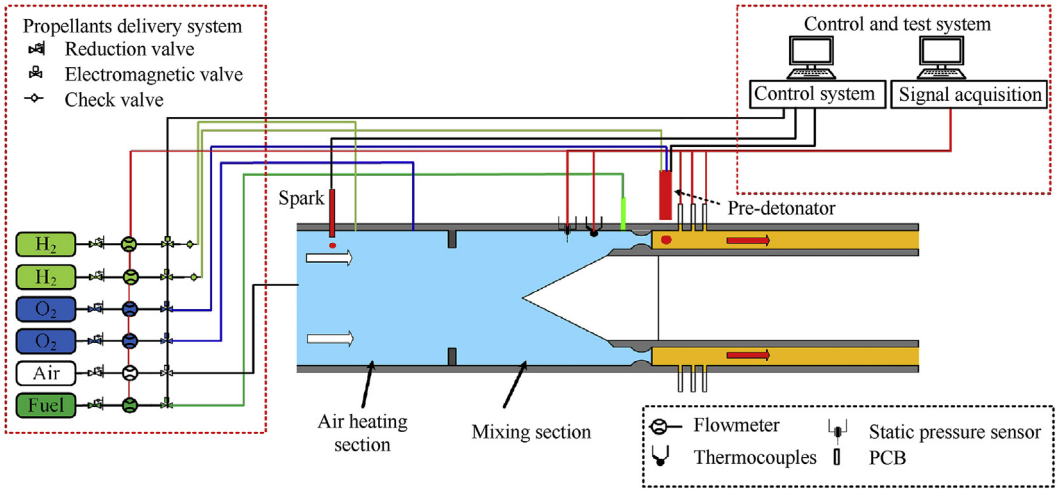

Fig. 1. Expermental system diagram.

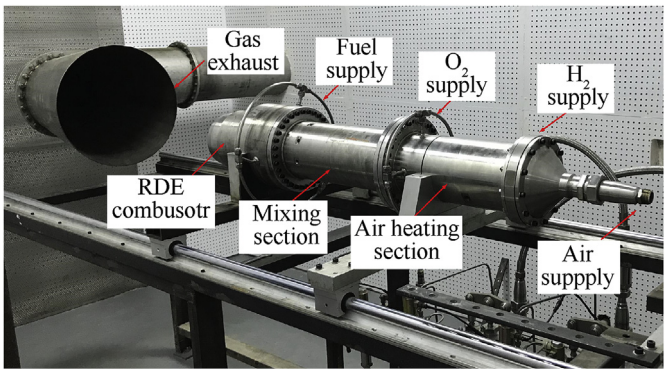

Fig. 2. Photograph of the two-pahse RDC test system.

2.2. Measurement methodology

As shown in Fig. 3, the piezoelectric sensors (Model: PCB113B26) are flush-mounted in the out wall of the combustor. The three PCB sensors are installed in an axial cross section, the azimuth of PCB1 is defined as 0°, PCB2 and PCB3 are located at 60° and 240° respectively. The sampling frequency of PCB sensors is 200 kHz, and the rise time is less than 1.0 μs. The mass flow rates of air, hydrogen, oxygen and kerosene are measured by Endress + Hauser mass flowmeter. The maximum errors of mass flowmeter is ±0.35%. To analysis the propagation characteristics of rotating detonation wave, high-frequency pressure transducers are used in the experiment. The static pressure transducers (Omega-PX419) with an accuracy of ±0.08% are used to record static pressures in propellant manifolds. The thermocouple with an accuracy of $\pm(0.15 + 0.002|T|)$°C installed near the air inlet of the annular combustor is used to measure the temperature of the oxygen-enriched air during the RDC operation.

2.3. Time sequence

All the experimental tests are performed sequentially, as shown in Fig. 4. During the tests, the acquisition system is triggered to capture the high frequency pressure oscillation in the combustor. Then air, hydrogen and oxygen are injected into air-heater simultaneously, the spark plug of air-heater is triggered before hydrogen and oxygen. The propellant is injected into RDC combustor, and the pre-detonator starts filling H_2 and O_2. After the H_2/O_2 supply is turned off, the spark plug of the pre-detonator ignite the mixture. The propellant in the RDC is ignited by the detonation wave generated in the pre-detonator. When the experiment process is finished, the main propellant, H_2/O_2, air and acquisition system are closed in sequence.

3. Results and discussion

A series of experiments are performed to study the effects of oxygen-enriched air temperature on the instabilities of the two-phase RDC. T is the total temperature of the oxygen-enriched air; $\dot{m}_{gas}$denotes the sum of mass flow rates of air, O_2 and H_2; $\dot{m}_{fuel}$is the mass flow rate of kerosene. ϕ_{O_2} and φ denote the mass fraction of O_2 and the equivalent ratio of the mixture, respectively. The mass fraction of O_2 and the equivalent ratio were determined by the following formulas:

$$\phi_{O_2} = \frac{0.23\dot{m}_{air} + \dot{m}_{o_2} - 8\dot{m}_{H_2}}{\dot{m}_{air} + \dot{m}_{o_2} + \dot{m}_{H_2}} \quad (1)$$

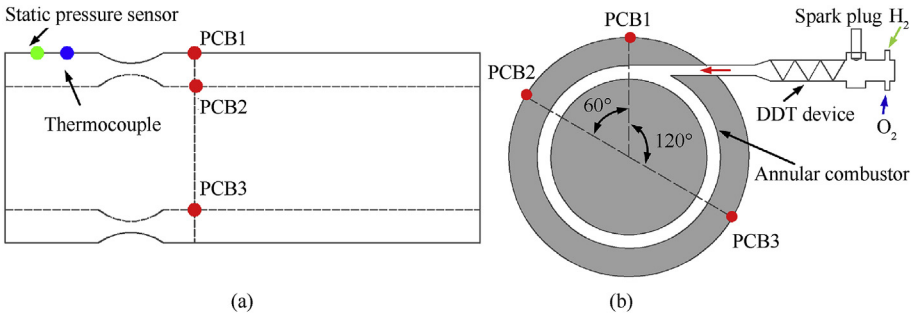

Fig. 3. (a) Locations of the sensors; (b) pre-detonator.

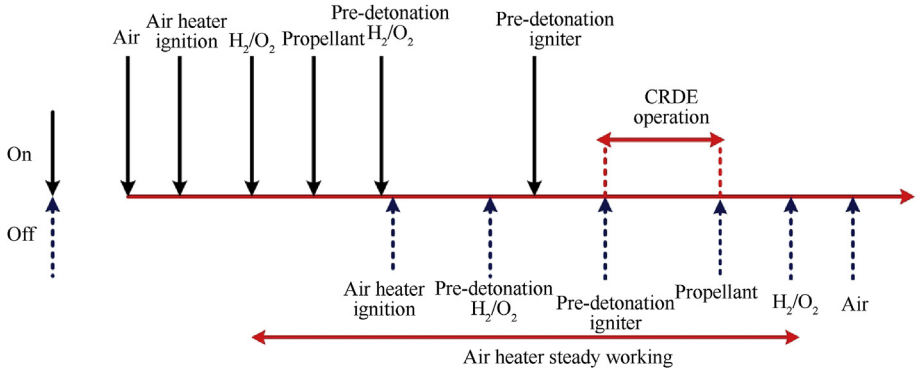

Fig. 4. Time sequence of experimental test.

$$\varphi = \frac{\left(\dot{m}_{\mathrm{fuel}}/\dot{m}_{\mathrm{air}}\right)_{\mathrm{real}}}{\left(\dot{m}_{\mathrm{fuel}}/\dot{m}_{\mathrm{air}}\right)_{\mathrm{stoi}}} \tag{2}$$

Here, $\dot{m}_{\mathrm{air}}$is the air mass flow rate and $\dot{m}_{\mathrm{o_2}}$ is the O_2 mass flow rate. $\dot{m}_{\mathrm{H_2}}$is the mass flow rate of H_2. By simultaneously increasing the mass flow of hydrogen and oxygen entering the air-heater, the total temperature of oxygen-enriched air is changed from 620 K to 870 K. The mass fraction of O_2 was set at about 35%, the mass flow rate of oxygen-enriched air was about 1000 g/s, and the mass flow rate of kerosene remained constant in a series of experiments.

3.1. Operation process

Fig. 5(a) shows the static pressure and temperature curves in the air-heater, when the RDC is operating at $\dot{m}_{\mathrm{gas}} = 1006.0$ g/s, $\phi_{O_2} = 0.35$, $\varphi = 0.81$. At the initial time, air and oxygen are injected into the air-heater, and the static pressure in the air-heater begins to rise. When $t = 0.6$ s, hydrogen is injected and ignited by a spark plug. The static pressure and temperature in the air-heater rise rapidly. When $t = 2.58$ s, the mixture of liquid kerosene and oxidizer is ignited, forming a two-phase RDW propagating in the RDC, as shown in Fig. 5(b). The increase of static pressure in air-heater is relate to the system upstream of the combustor adjusting to the effects of the rotating detonation waves. During the RDC operation, the total temperature of the incoming air is stable at about 620K. When $t = 3.51$ s, the supplies of kerosene, hydrogen and oxygen are shut off by the reversing valves. The pressure and temperature in air-heater decreases sharply while the air continues to supply for 6 s. The operation time of the RDC is about 930 ms, which is sufficient to form self-sustained RDW and to analyze its propagation characteristics.

The original signals are converted by high pass filtering to remove the spurious thermal shift and get a visualized view [12], as shown in Fig. 5(b). It can be seen that the self-sustained RDW is formed after the pre-detonation wave enters the combustor. The average pressure peaks of the rotating detonation wave are about 0.5 MPa. Fig. 5(c) shows the STFT results of the PCB1 pressure signal. A well-defined line appears at $f = 2148$ Hz, which indicates that the test converges to a relatively stable operating frequency. The corresponding average velocity is 1031.9 m/s. The deficit of the detonation velocity is affected by various factors such as the lateral expansion, blending of fuel and oxidizer and the evaporation of kerosene droplets. At the time of 3.32 s, the engine enters the quenching process, and the propagation frequency of the detonation wave shows a downward trend with time, and finally completely extinguishes at 3.63 s.

3.2. Temporal and spatial instability

Fig. 6 shows the pressure histories curve measured by PCB1 and the instantaneous propagation velocity of detonation wave from 3038 ms to 3048 ms. The instantaneous propagation velocity can be obtained by:

$$v_i = \pi D_0 f_i / N \tag{3}$$

where D_0 is the combustor outer diameter, and N is the number of RDW.

The RDW propagation velocity oscillates around the average propagation velocity of 1030 m/s. It can be found that the detonation wave pressure peaks and velocity are relatively stable from 3038 ms to 3041 ms. When $t = 3042$ ms, the phenomenon that the strong detonation wave and weak detonation wave appear alternately and regularly. There are four pressure spikes presented in Fig. 6. Correspondingly, the propagation velocity of detonation wave fluctuates periodically with the pressure peak of detonation wave. The stronger the detonation wave is, the faster the detonation wave propagates. This instability is probably caused by the interaction between detonation wave and supply plenum [22,24].

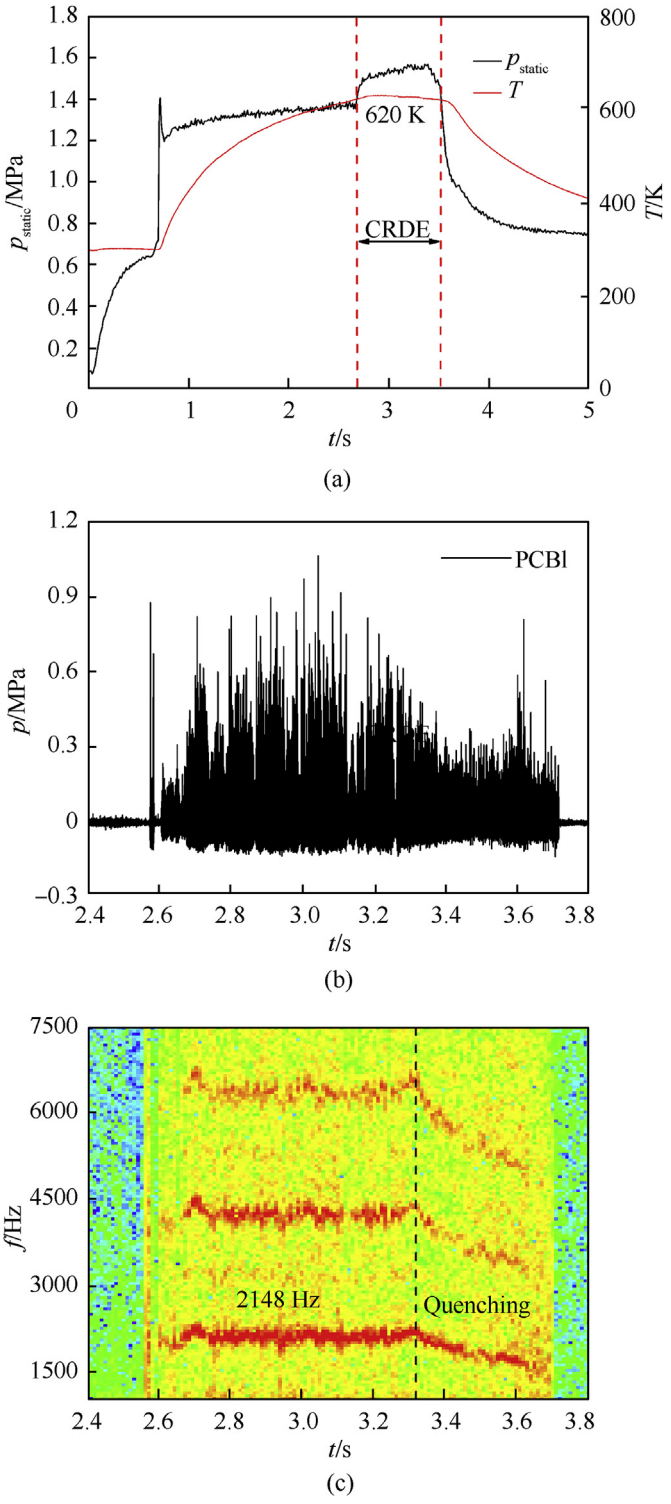

Fig. 5. The test results of operating at $\dot{m}_{\mathrm{gas}} = 1006.0$ g/s, $\phi_{O_2} = 0.35$, $\varphi = 0.81$. (a) Static pressure and temperature in air-heater; (b) High-frequency pressure signals by PCB1; (c) STFT frequency distribution.

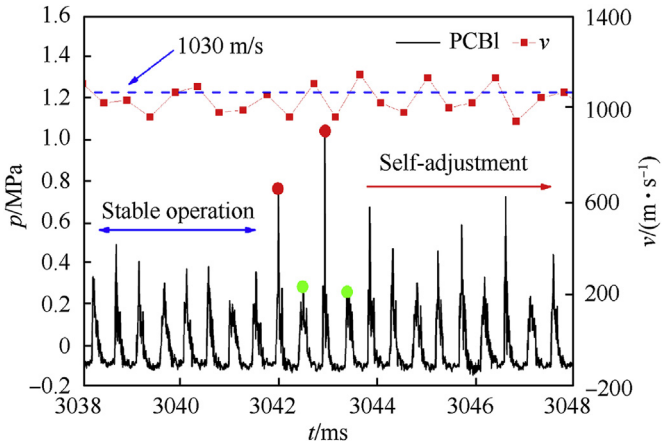

Fig. 6. Local view of high-frequency dynamic pressures of $T = 620$ K, $\dot{m}_{gas} = 1006.0$ g/s, $\phi_{O_2} = 0.35$, $\varphi = 0.81$.

After the strong detonation wave swept, the pressure at this position stays in a relatively high value for a longer time, and the propagation velocity of the strong detonation wave is relatively high. The filling process of the fresh combustible gas layer can be resumed only when the pressure of the detonation wave sweeping position is reduced. This results in a shorter filling time and a thinner thickness of the combustible gas layer. The mass flow rate of combustible mixture passing through the intake ring gap decreases, and the energy content released by the combustible mixture participating in detonation combustion decreases, resulting in a decrease in detonation wave pressure and velocity [44]. After a period of self-adjustment, the RDW can resume stable self-sustained propagation [45].

Fig. 7 is the local view of the high frequency pressure curve measured by PCB at different locations in the circumference of the same section. From the periodical oscillation that can be clearly recognized, it is judged that the RDW propagates in single wave counter-clockwise mode. Fig. 7(a) shows that the RDW propagates in the combustor for 8 cycles in the period of 2636 ms–2640 ms. In the same circle, the pressure peaks of RDW at the position of PCB3 are obviously higher than that at the other two positions. Detonation wave intensity increases each time it passes through PCB3 and weakest in the position of PCB1. Fig. 7(b) reveals that the pressure peaks of RDW is consistent at different locations. This indicates that the mixing of fuel and oxidizer is uniform sufficiently in different positions of RDC during this time. Fig. 7(c) shows that the intensity of RDW at the position of PCB1 strengthens every time it passes through, and weakest at the position of PCB3. Compared with Fig. 7(a), the spatially varying pressure oscillation exhibits the reverse order. The spatially non-homogenous oscillation can be characterized by a given sector of the RDC exhibits significantly higher pressure peaks (subsequent detonation cycles) than other sectors within a given time window [49].

3.3. Mode transition

We find the phenomenon of single-double-single wave transition at $T = 732$ K, $\dot{m}_{gas} = 997.4$ g/s, $\phi_{O_2} = 0.35$ and $\varphi = 0.81$. The red rectangles in Fig. 8(a) represent the single-double-single wave transition positions, and four mode transitions have occurred.

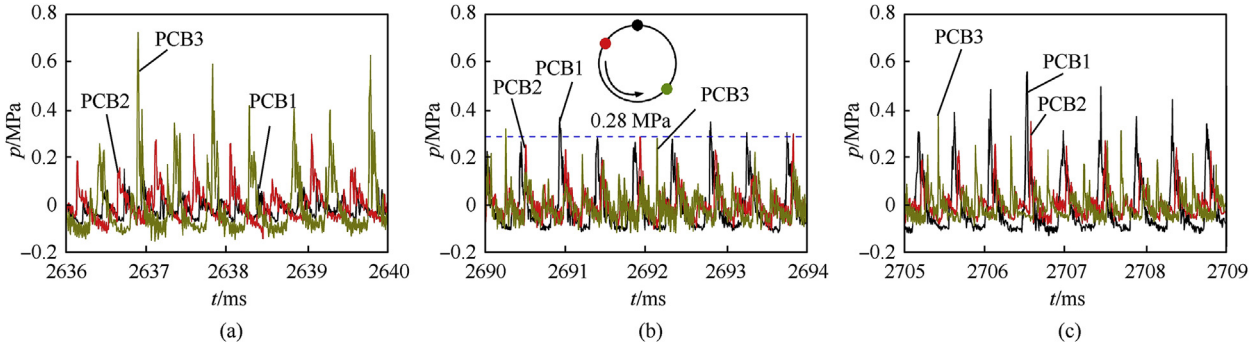

Fig. 7. Pressure evolution of different circumferential positions of $T = 620$ K, $\dot{m}_{gas} = 1006.0$ g/s, $\phi_{O_2} = 0.35$, $\varphi = 0.81$.

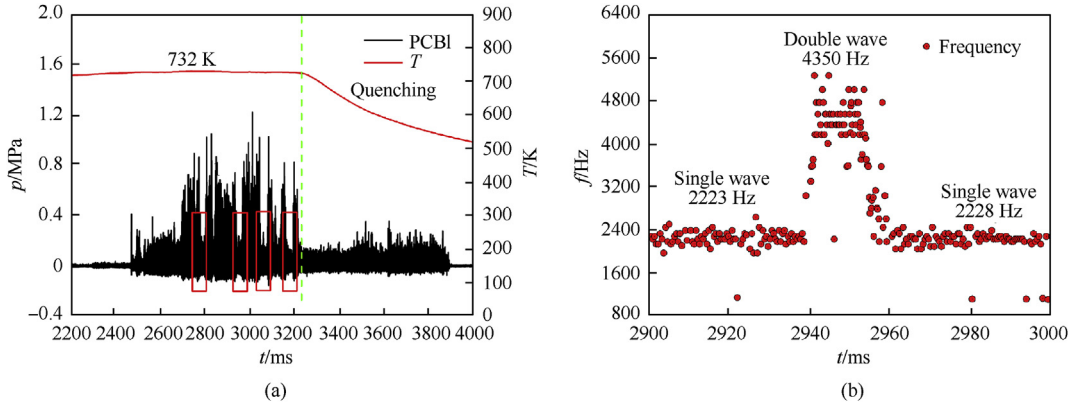

Fig. 8. The test results of operating at $T = 732$ K, $\dot{m}_{gas} = 997.4$ g/s,$\phi_{O_2} = 0.35$, $\varphi = 0.81$.(a) The distribution of pressure and temperature with time; (b) The distribution of frequency with time.

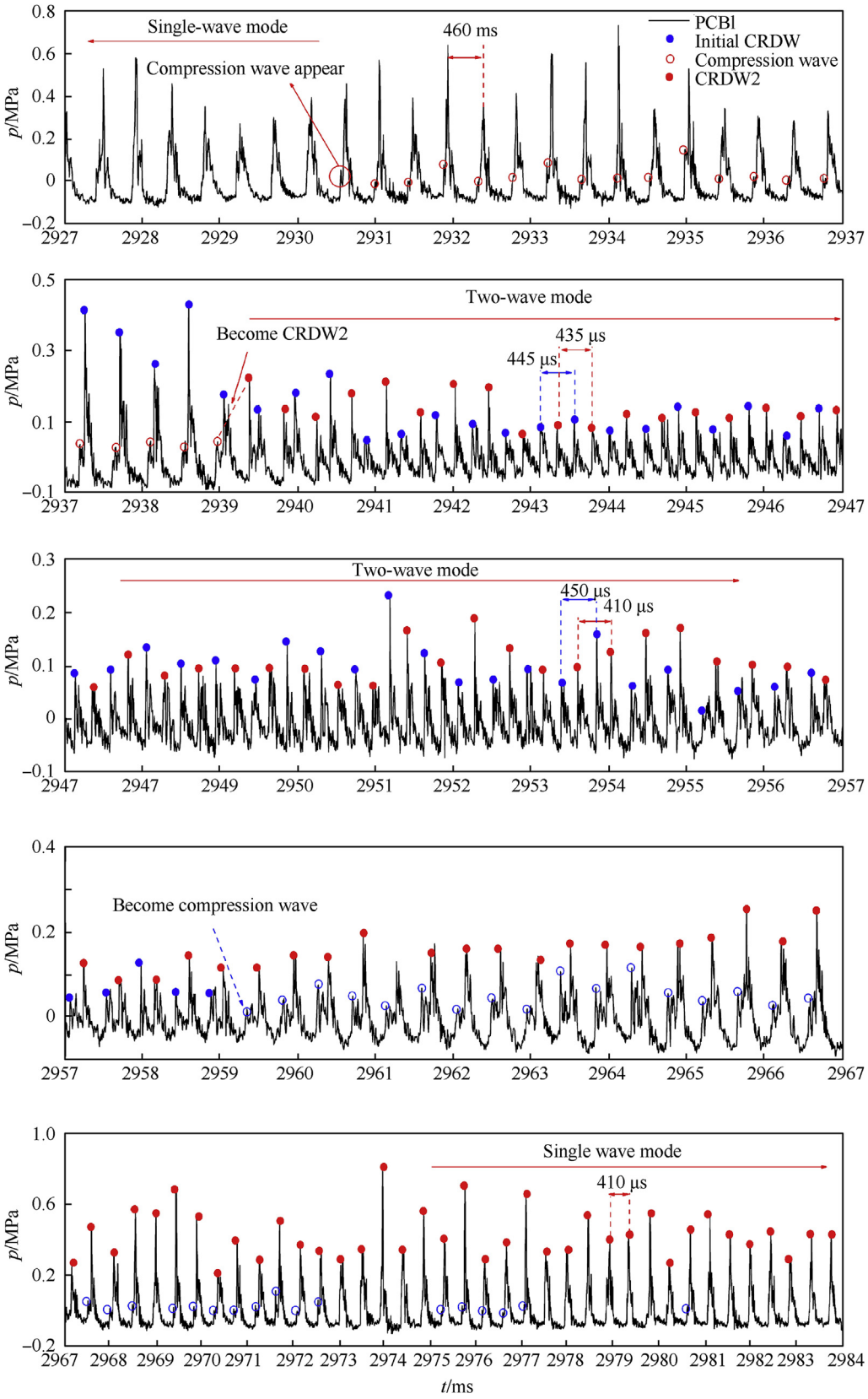

Fig. 9. Local view of high-frequency dynamic pressures in one of the transition areas.

Fig. 8(b) shows the distribution of frequency with time in one of the transition areas. When RDC operates in single-wave mode, the propagation frequencies of RDW are 2223 Hz and 2228 Hz, the corresponding propagation velocities are 1067.9 m/s and 1070.3 m/s, respectively. In double-wave mode, the propagation frequency is 4350 Hz, which is about twice that of single-wave mode.

Fig. 9 presents the local view of the pressure histories in one of the transition areas. The weaker compression wave emerges before the initial detonation wave, and the propagation direction is the same. The propagation period of the initial detonation wave is 460 μs, and the corresponding propagation velocity is 1044.4 m/s. The appearance of the compression wave is mainly due to the pressure fluctuation in the RDC, which leads to a smaller pressure peak earlier than the initial detonation wave. The compression wave contacts the fresh combustible gas layer in advance before the initial detonation wave, absorbing more energy, and the pressure peak and propagation speed gradually increase, resulting in the weakening of the initial detonation wave. Under the influence of compression wave, the initial detonation wave intensity is weaken, and the pressure peaks of RDW are reduced. At $t = 2939$ ms, the compression wave develops into a new rotating detonation wave (RDW2). The instantaneous propagation velocity of RDW2 is 1090.9 m/s, and the propagation velocity of initial detonation wave is 1054.9 m/s. The propagation velocity of RDW2 is slightly larger than the initial detonation wave.

The interval between the two detonation waves is 220 μs, and the corresponding distance is about 236 mm, which is about half the circumference of the combustion chamber. The engine works in the double-wave homo-rotating mode from 2940 ms to 2959 ms. The double-wave mode cannot stably self-sustained for a long time. The leading shock wave and reaction zone of initial detonation wave slowly decoupled and became a compression wave around 2959 ms, gradually weakening until it disappears at 2973 ms, and RDW2 gradually increased until it stably propagated. The propagation velocity of RDW2 is basically the same as the previous initial detonation wave. During the subsequent propagation of RDW2, there will be new compression waves, and the single-double-single wave transition areas will appear again.

The reason for the emergence of RDW2 is that the origin of compression wave may be pressure fluctuation in the RDC. The possibility of pressure fluctuation mainly includes: (1) the compression wave generated by the reflection of the detonation wave due to the influence of the curvature of the inner and outer walls of the combustor; (2) the compression wave generated by the RDW being stripped by the ignition hole or pressure measurement hole on the outer walls of the combustor; (3) The compression wave generated by oblique shock wave from components that are not completely combusted in the high-temperature product area.

The process of single-double-single wave transition can be divided into four states: (I) The compression waves emergence; (II) Compression waves strengthen to be a new detonation wave; (III) Sustain double wave; (IV) Initial detonation wave weaken to disappear. An increase in the total temperature of the oxygen-enriched air results in an enhanced activity of the fresh combustible mixture, which contributes to the compression wave acceleration and the combination of shock wave with its corresponding chemical reaction zone. It is consistent with the characteristics of deflagration-to-detonation (DDT) in flow field summarized by Oran et al. [46]. Therefore, we speculate that the formation of the new RDW is the result of DDT caused by the chemical reaction at the contact surface.

3.4. Re-initiation

The re-initiation phenomenon was found at the $T = 870$ K,

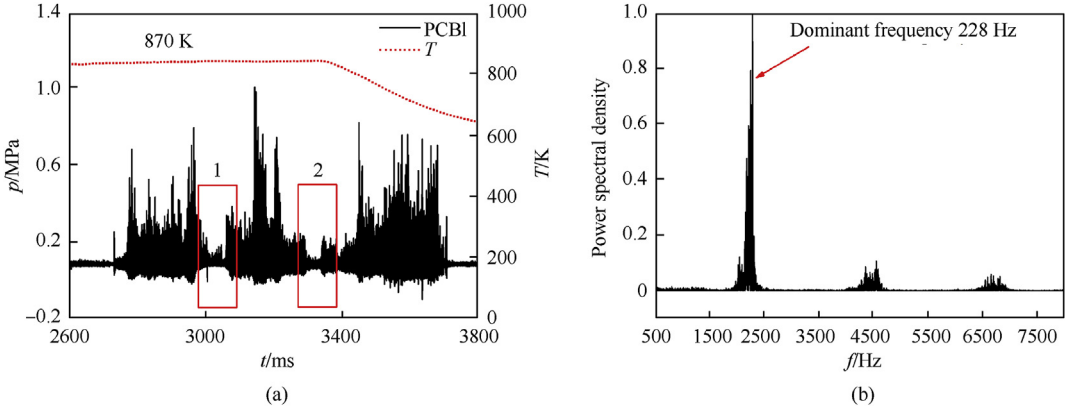

Fig. 10. The test results of operating at $T = 870$ K, $\dot{m}_{gas} = 1014.8$ g/s, $\phi_{O_2} = 0.35$, $\varphi = 0.81$.(a) The distribution of pressure with time; (b)FFT frequency distribution.

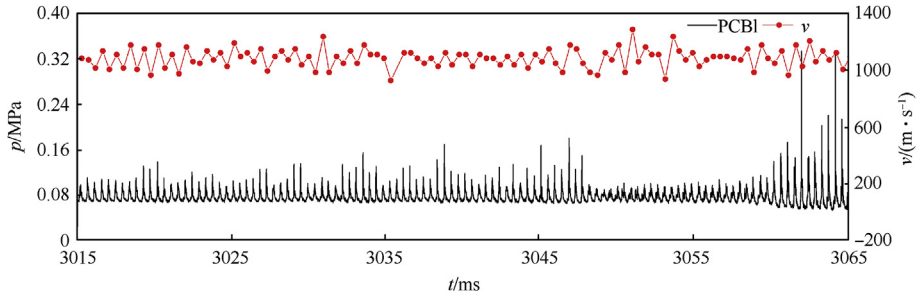

Fig. 11. Local view of the pressure and velocity distribution in the first rectangle.

$\dot{m}_{gas}$ = 1014.8 g/s, ϕ_{O_2} = 0.35, φ = 0.81. From the high-frequency pressure distribution, it can be found that there are two quenching phenomena during RDC operation, which are marked with red rectangles in Fig. 10(a). The high-frequency pressure distribution in the two rectangular areas is shown in Fig. 11 and Fig. 12, respectively.

As shown in Fig. 11, it can be seen that the pressure peaks of the RDW are relatively lower at 3015 ms–3065 ms, but it can still maintain self-sustained propagation. The average propagation velocity is about 1076.3 m/s, and the corresponding propagation frequency is 2240 Hz. As shown in Fig. 10(a), we can see that the peak pressure of the detonation wave before 3015 ms is higher. Under high temperature conditions, RDW has a weak adaptive adjustment ability after experiencing a strong detonation wave process, resulting in a lower peak pressure at this stage and requiring longer recovery time. At t = 3048 ms, the phenomenon that the leading shock wave separated from the reaction zone appeared. After the pressure in the RDC decreased, the filling process of the combustible gas layer resumed, and the RDW increased again. This is consistent with the FFT analysis results in Fig. 10(b), indicating that the RDC has not stopped working at this stage.

Fig. 12 shows the pressure distribution in the second rectangle. At t = 3215 ms, a weak compression wave following the RDW was observed. Due to the weak compression wave, the fresh mixture in the front of RDW decreases and the RDW weakens in the next cycle. The weakening of the detonation wave leads to an increase in the intensity of the compression wave in the next cycle. In this test, the weak compression wave did not form a new RDW (similar to the test of T = 732 K, $\dot{m}_{gas}$ = 997.4 g/s, ϕ_{O_2} = 0.35, φ = 0.81), but resulted in the phenomenon of deflagration and detonation coexisting in the RDC. Before the re-initiation, a 31 ms deflagration mode was observed in the RDC. After a DDT process, RDC did not directly form a self-sustained RDW, but the coexistence of strong & weak detonation appeared. The relatively weaker RDW could not be self-sustained propagation, and the phenomenon of deflagration and detonation coexisted in RDC. Finally, after the transition process, a stable detonation wave was formed in the combustion chamber. The propagation period of the stable detonation wave is about 470

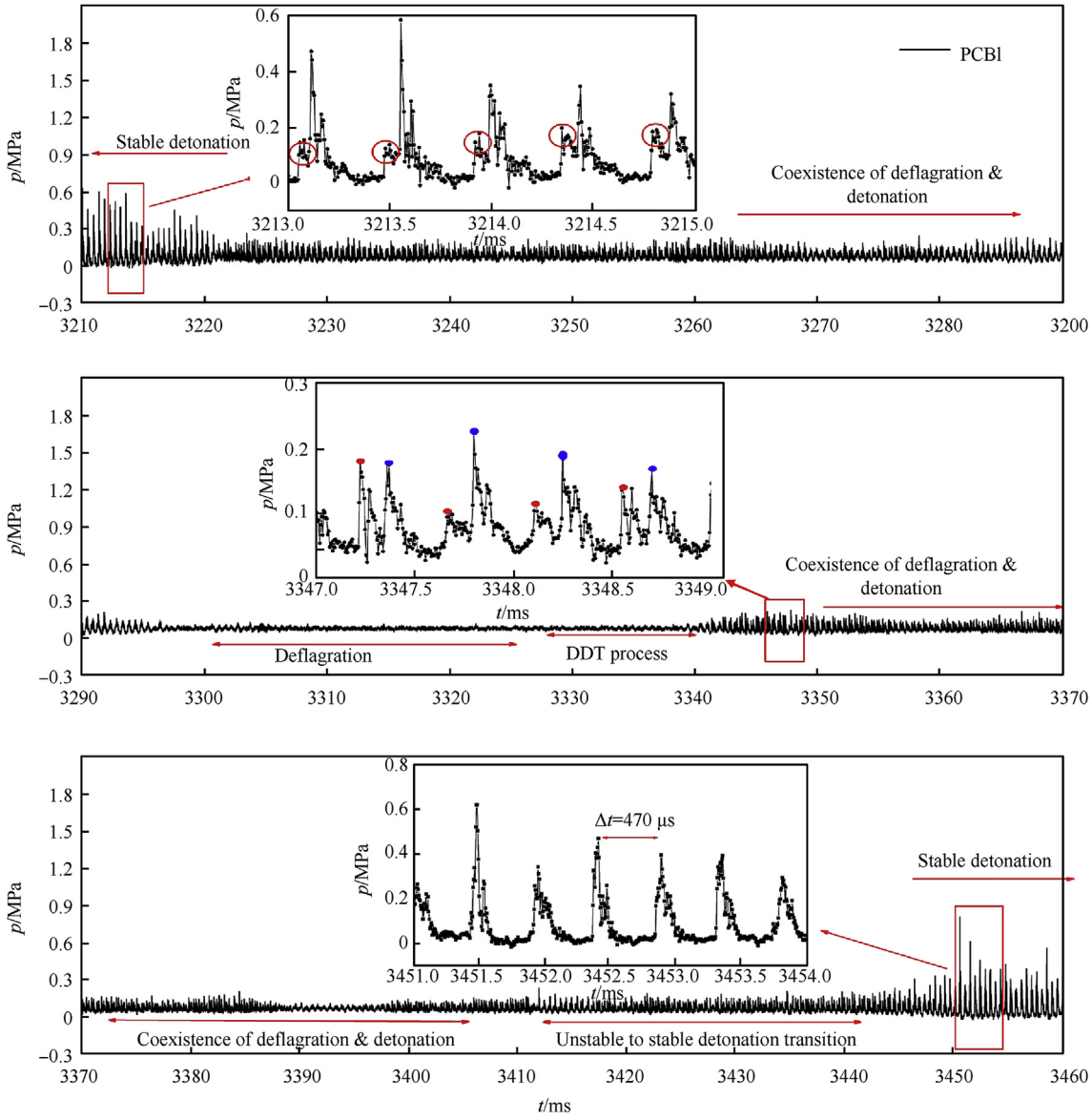

Fig. 12. Local view of the pressure distribution in the second rectangle.

μs, and the corresponding propagation velocity is 1022.2 m/s. The entire re-initiation process of the RDC includes DDT process, coexistence of strong & weak detonation, unstable to stable detonation transition and stable detonation [47,48].

With the increase of the oxygen-enriched air total temperature, the deflagration on the contact surface between the combustion products and the fresh gas layer is enhanced [50]. Deflagration consumes fresh combustible gas before the detonation wave, which is detrimental to the self-sustained propagation of the RDW. As for the reason for the re-initiation phenomenon, since the combustible mixture is sufficiently active, the RDC tends to develop a self-sustained RDW through the DDT process.

4. Conclusions

In this paper, the room-temperature liquid kerosene is selected as fuel and the preheated oxygen-enriched air is the oxidizer. Under the condition of equivalence ratio of 0.81 and oxygen mass fraction of 0.35, the experimental tests of RDC were carried out to study the instability propagation characteristics of RDW. The results are concluded as follows:

(1) Under the condition of 620 K, a self-sustained propagation two-phase RDW is obtained, and the average propagation velocity is about 1030 m/s. During the propagation of RDW, the pressure peaks and velocity will alternate in a short time. This instability is mainly due to the interaction between RDW and supply plenum. Furthermore, the inconsistent mixing of fuel and oxidizer at different circumferential positions is related to RDW oscillate spatially.
(2) The phenomenon of single-double-single wave transition is found in the experiment where the total temperature of oxygen-enriched air is 732 K. During the transition, the initial RDW weakens until disappears, and the compression wave strengthens until it becomes a new RDW and propagates steadily. The compression wave has the potential to trigger DDT and form a new RDW.
(3) The quenching and re-initiation phenomenon occurs at 870 K oxidizer temperature. The excessive high temperature of the oxygen-enriched air, the deflagration on the contact surface between the combustion products and the fresh gas layer will enhance, which can induce the quenching in the RDC. On the other hand, the increase of propellant activity due to high temperature contributes to the RDC re-initiated through the DDT process.

Declaration of competing interest

No conflict of interest exits in the submission of this manuscript, and manuscript is approved by all authors for publication.

Acknowledgments

This work was supported by the National Natural Science Foundation of China (Grant No. 11802137, 11702143 and 11802039) and the Fundamental Research Funds for the Central Universities(No.30919011259).

References

[1] J.H.S. Lee, The detonation phenomenon, Cambridge University Press2008.
[2] Heiser W, Pratt D. Thermodynamic cycle analysis of pulse detonation engines. J Propul Power 2002;18:68–76.
[3] Wolański P. Detonation propulsion. Proc Combust Inst 2013;34:125–58.
[4] Yi TH, Lou J, Turangan C, Choi JY, Wolański P. Propulsive performance of a continuously rotating detonation engine. J Propul Power 2011;27:171–81.
[5] Hishida M, Fujiwara T, Wolański P. Fundamentals of rotating detonations. Shock Waves 2009;19(1):1–10.
[6] Wolański P. Application of the continuous rotating detonation to gas turbine. Appl Mech Mater 2015;782:3–12.
[7] Anand V, Gutmark E. Rotating detonation combustors and their similarities to rocket instabilities. Prog Energy Combust Sci 2019;73:182–234.
[8] Nordeen CA, Schwer D, Schauer F, Hoke J, Barber T, Cetegen BM. Role of inlet reactant mixedness on the thermodynamic performance of a rotating detonation engine. Shock Waves 2015;26:1–12.
[9] Schwer D, Kailasanath K. Numerical investigation of the physics of rotating-detonation-engines. Proc Combust Inst 2013;34:1991–8.
[10] Paxson DE. Examination of wave speed in rotating detonation engines using Simplified Computational Fluid dynamics. 2018. AIAA Paper, 2018-1883.
[11] Hishida M, Fujiwara T, Wolański P. Fundamentals of rotating detonations. Shock Waves 2009;19:1–10.
[12] Zhang H, Liu W, Liu S. Effect of inner cylinder length on H_2/air rotating detonation. Int J Hydrogen Energy 2016;41:13281–93.
[13] Zhang H, Liu W, Liu S. Experimental investigations on H_2/air rotating detonation wave in the hollow chamber with Laval nozzle. Int J Hydrogen Energy 2017;42:3363–70.
[14] Tang XM, Wang JP, Shao YT. Three-dimensional numerical investigations of the rotating detonation engine with a hollow combustor. Combust Flame 2015;162:997–1008.
[15] Bykovskii FA, Zhdan SA, F Vedernikov E, N Samsonov A, S Zintsova A. Detonation combustion of a hydrogen-oxygen mixture in a plane-radial combustor with exhaustion toward the center. Combust Explos Shock Waves 2016;52:446–56.
[16] Kindracki J. Experimental research on rotating detonation in liquid fuel-gaseous air mixtures. Aero Sci Technol 2015;43:445–53.
[17] M Li J, Chang PH, Lei L, Yang Y, Teo CJ, C Khoo B. Investigation of injection strategy for liquid-fuel rotating detonation engine. 2018. AIAA Paper, 2018-0403.
[18] A Bykovskii F, Zhdan SA, Vedernikov EF, Zholobov YA. Detonation combustion of coal, explos. Shock Waves 2012;48:203–8.
[19] St George A, Anand V, Driscoll R, Gutmark E. A correlation-based method to quantify the operating state in a rotating detonation combustor. 2016. AIAA Paper 2016-1402.
[20] Anand V, St George A, Gutmark E. Amplitude modulated instability in reactants plenum of a rotating detonation combustor. Int J Hydrogen Energy 2017;42:12629–44.
[21] Li B, Wu Y, Weng C, Zheng Q, Wei W. Influence of equivalence ratio on the propagation characteristics of rotating detonation wave. Exp Therm Fluid Sci 2018;93:366–78.
[22] Anand V, St George A, Driscoll R, Gutmark E. Characterization of instabilities in a rotating detonation combustor. Int J Hydrogen Energy 2015;40:16649–59.
[23] Xie Q, Wen H, Li W, Ji Z, Wang B, Wolański P. Analysis of operating diagram for H2/Air rotating detonation combustors under lean fuel condition. Energy 2018;151:408–19.
[24] Anand V, St George A, Driscoll R, Gutmark E. Analysis of air inlet and fuel plenum behavior in a rotating detonation combustor. Exp Therm Fluid Sci 2016;70:408–16.
[25] Schwer DA, Kailasanath K. Feedback into mixture plenums in rotating detonation engines. AIAA Paper 2012-0617; 2012.
[26] Schwer DA, Kailasanath K. On reducing feedback pressure in rotating detonation engines. 2013. AIAA Paper 2013-1178.
[27] Liu S, Liu W, Lin Z, Lin W. Experimental research on the propagation characteristics of continuous rotating detonation wave near the operating boundary. Combust Sci Technol 2015;187:1790–804.
[28] Roy A, Ferguson DH, Sidwell T, O'Meara B, Strakey P, Bedick C, et al. Experimental study of rotating detonation combustor performance under Preheat and Back pressure operation. 2017. AIAA Paper, 2017-1065.
[29] Anand V, St George A, Driscoll R, Gutmark E. Investigation of rotating detonation combustor operation with H_2-Air mixtures. Int J Hydrogen Energy 2016;41:1281–92.
[30] Rankin BA, Richardson DR, Caswell AW, Naples AG, Hoke JL, Schauer FR. Chemiluminescence imaging of an optically accessible non-premixed rotating detonation engine. Combust Flame 2017;176:12–22.
[31] Frolov SM, Aksenov VS, Ivanov VS, Shamshin IO. Large-scale hydrogen-air continuous detonation combustor. Int J Hydrogen Energy 2015;40. 1616-1523.
[32] Lin W, Zhou J, Liu S, Lin Z, Zhuang F. Experimental study on propagation mode of H_2/Air continuously rotating detonation wave. Int J Hydrogen Energy 2015;40:1980–93.
[33] Kindracki J. Experimental studies of kerosene injection into a model of a detonation chamber. J. Power Technol. 2012;92:80–9.
[34] A Bykovskii F, Zhan A S. Continuous spin detonation of fuel air mixtures, Explos. Shock Waves 2006;42:463–71.
[35] Frolov SM, Aksenov VS, Ivanov VS, Shamshin IO. Continuous detonation combustion of ternary "hydrogen liquid propane air" mixture in annular combustor. Int J Hydrogen Energy 2017;42:16808–20.
[36] Wang D, Zhou J, Lin Z. Experimental investigation on operating characteristics of two phase continuous rotating detonation combustor fueled by kerosene. Propulsion Technology 2017;38:471–80.
[37] Zheng Q, Weng C, Bai Q. Experimental study on effects of equivalence ratio on detonation characteristics of liquid-fueled rotating detonation engine.

Propulsion Technology 2015;36:947–52.
[38] Zhong Y, Wu Y, Jin D, Chen X, Yang X, Wang S. Investigation of rotating detonation fueled by pre-combustion creaked kerosene. Aero Sci Technol 2019;95:105480.
[39] Zhong Y, Wu Y, Jin D, Chen X, Yang X, Wang S. Effect of channel and oxidizer injection slot width on the rotating detonation fueled by pre-combustion cracked kerosene. Acta Astronaut 2019;165:365–72.
[40] Xie Q, Wang B, Wen H, He W, Wolański P. Enhancement of continuously rotating detonation in hydrogen and oxygen-enriched air. Proc Combust Inst 2019;37:3425–32.
[41] St George A, Driscoll R, Anand V, Gutmark E. On the existence and multiplicity of rotating detonations. Proc Combust Inst 2017;36:2691–8.
[42] Gaillard T, Davidenko D, Dupoirieux F. Numerical optimization in non-reacting conditions of the injector geometry for a continuous detonation wave rocket engine. Acta Astronaut 2015;111:334–44.
[43] Zhou S, Ma H, Li S, Zhou C, Liu D. Experimental study of a hydrogen-air rotating detonation engine with variable air-inlet slot. Int J Hydrogen Energy 2018;43:11253–62.
[44] Peng L, Wang D, Wu X, Ma H, Yang C. Ignition experiment with automotive spark on rotating detention engine. Int J. Hydrogen Energy 2015;40:8465–74.
[45] Liu Y, Wang Y, Li Y, Li Y, Wang J. Spectral analysis and self-adjusting mechanism for oscillation phenomenon in hydrogen-oxygen continuously rotating detonation engine, Chin. J. Aeronaut. 2015;28:669–75.
[46] Oran ES, Gamezo VN. Origins of the deflagration-to-detonation transition in gas-phase combustion. Combust Flame 2007;148:4–47.
[47] Ma Z, Zhang S, Luan M, Yao S, Xia Z, Wang J. Experimental research on ignition, quenching, reinitiation and the stabilization process in rotating detonation engine. Int J Hydrogen Energy 2018;43:18521–9.
[48] Wang Y, Wang J. Coexistence of detonation with deflagration in the rotating detonation engines. Int J Hydrogen Energy 2016;41:14302–9.
[49] Anand V, Gutmark E. Types of low frequency instabilities in rotating detonation combutors. Active Flow and Combustion Control 2018:197–213.
[50] Lu FK, Mizener AR, Rodi PE. A study of integration of a rotating detonation engine to a waverider forebody. ISSW32; 2019.